Available online at www.sciencedirect.com
SCIENCE DIRECT®
ELSEVIER
Mechanism and Machine Theory 39 (2004) 603–619
Mechanism and Machine Theory
www.elsevier.com/locate/mechmt

Development and validation of a three-dimensional kinematic model for the McPherson steering and suspension mechanisms

Daniel A. Mántaras [a,*], Pablo Luque [a], Carlos Vera [b]

[a] Área de Ingeniería e Infraestructura de los Transportes, Universidad de Oviedo, Campus de Viesques, s/n, 33203 Gijón, Spain
[b] Área de Ingeniería Mecánica, Universidad Politécnica de Madrid, José Gutiérrez Abascal 2, 28006 Madrid, Spain

Received 28 January 2003; received in revised form 16 December 2003; accepted 27 December 2003

Abstract

A three-dimensional model is presented of the kinematic behaviour of a McPherson-type steering suspension. A general approach is put forward to determine the main parameters (caster, camber, steer angle, ...) which influence the handling of the vehicle, in function of the operational factors of the system. The input data are, on the one hand, the suspension and steering geometry, and on the other, the travel of the strut and the turn of steering wheel steer, which is obtained through monitoring the vehicle. The model has been applied to a standard vehicle and the validity of the results has been proven.

Keywords: Computer simulation; Automotive suspension; McPherson; Three-dimensional kinematic model

1. Introduction

The McPherson suspension is the system currently employed in the vast majority in small and medium-sized cars. In its commonest configuration (Fig. 1), the suspension consists of a strut (S) rigidly connected to the wheel support, or knuckle (K). The upper part of the strut is joined to the body (B) by means of a flexible union formed by an elastic element and a thrust ball bearing, which allows the rotation of strut [1].

In the lower part of the suspension there is a wishbone (W), which joins the knuckle to the body. The union between the knuckle and the wishbone is made via a spherical joint (O'), the

* Corresponding author. Tel.: +34-985-181910; fax: +34-985-182433.
E-mail address: mantaras@correo.uniovi.es (D.A. Mántaras).

0094-114X/$ - see front matter
doi:10.1016/j.mechmachtheory.2003.12.006

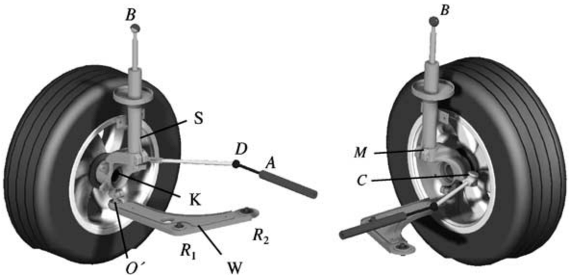

Fig. 1. Front and rear view of the characteristic parts of the right front wheel.

wishbone being connected to the body by means of two bushings (R_1 and R_2) which allow the relative rotation between both elements.

In order to transmit the turn of the steering wheel to the wheel, the tie rod is connected to the knuckle or the damper also by means of a spherical joint (Fig. 1).

Given the complexity of the system it is necessary to have access to analytical models which permit the optimisation of the global design of the vehicle [1–4]. In this paper we put forward a kinematic development which on the basis of the characteristics of the system allows us to determine its performance and to propose operational improvements.

2. Analysis of the real system

In the kinematic study of the McPherson-type steering suspension the following initial considerations have been taken into account [3]:

- it is assumed that all of the links which make up the suspension are rigid.
- deformations in the bushings are neglected.
- the effective radius of the wheel is determined in accordance with the dynamic characteristics of the tyre.

The kinematic analysis of the system corresponding to a road wheel reveals a total of seven elements: the body, the wishbone, the knuckle, the damper piston rod, the tie rod, the steering rack and the wheel. The kinematic joints for these elements are given in Table 1.

The degrees of freedom (d.o.f.) of the mechanism are calculated using the criteria of Kutzbach [5–8], according to the expression:

$$\begin{aligned}\text{d.o.f.} = {} & 6 \cdot (7\ \text{bodies} - 1) - 4(\text{spherical}) \cdot 3 - 2(\text{revolute}) \cdot 5 - 1(\text{translational}) \cdot \\ & 5 - 1(\text{cylindrical}) \cdot 4 = 5\end{aligned} \tag{1}$$

Of the five degrees of freedom, only two are representative of the kinematics of the wheel: the position of the steering rack and the travel of the strut.

If the analysis is extended to the model of the whole of the front axle, (Fig. 2) a total of three representative d.o.f. are found. That is to say, the kinematic behaviour of the whole mechanism

Table 1
Summary of the links and the joints which connect them

Joint	d.o.f.		Elements related by kinematic joints
Revolute	1	O	Body–wishbone
Spherical	3	O'	Wishbone–strut–knuckle
Spherical	3	C	Steering tie rod–strut–knuckle
Revolute	1	O_R	Wheel–strut–knuckle
Spherical	3	D	Steering rod–steering rack
Translational	1	A	Steering rack–body
Cylindrical	2	B–M	Piston rod–damper tube
Spherical	3	B	Body–McPherson strut

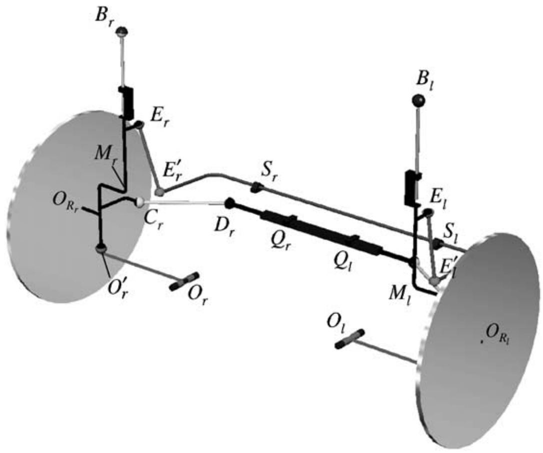

Fig. 2. Kinematic model of the McPherson-type suspension and rack-and-pinion steering.

can be found by way of the evaluation of three variables, namely the position of the steering rack (action upon the steering wheel) and the travel of the McPherson struts.

The turn of the steering wheel, that is to say the displacement of the rack, is controlled directly by the driver of the vehicle, whilst the travel of the suspension depends on dynamic actions, on the characteristics of the shock-absorbing and elastic elements of the suspension, on the suspension geometry, etc. These variables are easily measured in a vehicle instrumented with linear or angular displacement electronic sensors.

3. Reference frames used

One reference frame (moving) is considered for each wheel (Fig. 3), plus a global reference frame (non-moving or inertial) for the vehicle ($O^V xyz$).

The reference frame of the vehicle has its origin in the centre of gravity of the vehicle itself, and follows the notation proposed by ISO 8855, Fig. 3.

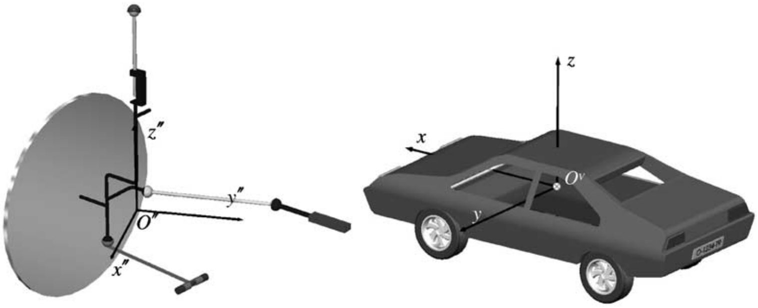

Fig. 3. Front wheel and vehicle (ISO 8855) reference frames.

The movable reference frame $O''x''y''z''$ is defined as the system linked to the strut–knuckle, with the $O''z''$-axis coinciding with the damper axis defined by points M and B. The $O''x''y''$ plane is defined by point C and the $O''x''$-axis is defined by points O'' and C.

The position and orientation of the suspension strut–knuckle in space can be defined by locating the origin of the body-fixed $O''x''y''z''$ frame and specifying an orthogonal direction cosine matrix that defines the orientation of the $O''x''y''z''$ frame [9]. The transformation matrix of the coordinates from the movable reference frame, system $O''x''y''z''$, to the frame of the vehicle, is offered below:

$$\mathbf{T}_{\mathbf{O^Vxyz}}^{\mathbf{Ox''y''z''}} = \begin{bmatrix} [\mathbf{B}] & \left\{\overrightarrow{\boldsymbol{O^V O''}}\right\} \\ 0 & 1 \end{bmatrix} \tag{2}$$

where the matrix $[\mathbf{B}]$ is a function of the three-dimensional orientations and $\{\overrightarrow{\boldsymbol{O^V O''}}\}$ is the vector from O^V to O''. The change in coordinates will be:

$$(x, y, z, 1) = \mathbf{T}_{\mathbf{O^Vxyz}}^{\mathbf{Ox''y''z''}} \cdot \begin{pmatrix} x'' \\ y'' \\ z'' \\ 1 \end{pmatrix} \tag{3}$$

The inverse transformation matrix will be:

$$\mathbf{T}_{\mathbf{Ox''y''z''}}^{\mathbf{O^Vxyz}} = \begin{bmatrix} [\mathbf{B}]^{-1} & -[\mathbf{B}]^{-1}\left\{\overrightarrow{\boldsymbol{O^V O''}}\right\} \\ 0 & 1 \end{bmatrix} \tag{4}$$

The matrix $[\mathbf{B}]$ is defined using the Euler parameters, which eliminate the drawbacks of other commonly used angular coordinates such as Euler angles and may, in many cases, substantially simplify the mathematical formulation [10–12].

The Euler's theorem said: if the origins of two right-hand Cartesian reference frames coincide, then they may be brought into coincidence by a single rotation (χ) about some axis ($\vec{w}$). So, the transformation matrix $[\mathbf{B}]$ expressed in terms of Euler parameters is on the form:

$$[\mathbf{B}] = 2\begin{bmatrix} \left(e_0^2+e_1^2-\frac{1}{2}\right) & (e_1e_2-e_0e_3) & (e_1e_3+e_0e_2) \\ (e_1e_2+e_0e_3) & \left(e_0^2+e_2^2-\frac{1}{2}\right) & (e_2e_3-e_0e_1) \\ (e_1e_3-e_0e_2) & (e_2e_3+e_0e_1) & \left(e_0^2+e_3^2-\frac{1}{2}\right) \end{bmatrix} \tag{5}$$

where e_0, e_1, e_2, e_3 are the Euler parameter defined as:

$$\begin{aligned} e_0 &= \cos\frac{\chi}{2} \\ e &= \begin{bmatrix} e_1 \\ e_2 \\ e_3 \end{bmatrix} = \vec{\boldsymbol{w}}\cdot\sin\frac{\chi}{2} \end{aligned} \tag{6}$$

4. Approach of the kinematic model

The methodology to determine the kinematic equations of each wheel in function of the travel of the strut and the rotation of the steering wheel, is based on the use of the three-dimensional constraint equations for the origin point of the movable reference frame [9,13], point O''. Having defined these point and the Euler parameters, the wheel plane and its direction vector are determined, which allows us to calculate the steering and suspension geometry.

It is assumed that the geometric parameters of the steering and suspension system, the coordinates of the characteristic points and the dimensions of the elements, are known. It is also assumed that the values of the variables associated with the degrees of freedom determined, the travel of the damper and the turn of steering wheel, can be measured in a real case.

4.1. Wishbone constraint equations

The wishbone is assumed as a revolute–spherical composite joint (Fig. 4).

Its analytical definition is that the distance between points O and O' is equal to the wishbone radius (R_w) and that vectors $\vec{\boldsymbol{u}}_\mathrm{w}$ and $\vec{\boldsymbol{d}}_{OO'}$ be orthogonal. That is:

$$\Phi^d(O', O, R_\mathrm{w}) = 0 \tag{7}$$

$$\Phi^p(\vec{\boldsymbol{u}}_\mathrm{w}, \vec{\boldsymbol{d}}_{OO'}) = 0 \tag{8}$$

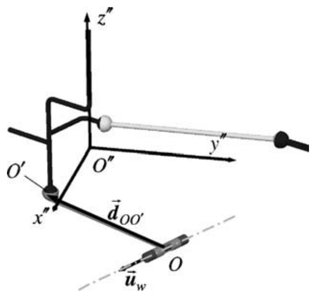

Fig. 4. Revolute–spherical composite joint.

where $\vec{\boldsymbol{d}}_{OO'}$ is:

$$\vec{\boldsymbol{d}}_{OO'} = \vec{\boldsymbol{r}}_{O^V O''} + [\mathbf{B}] \cdot \vec{\mathbf{s}}^{\mathrm{T}}_{O''O'} - \vec{\boldsymbol{r}}_{O^V O} \tag{9}$$

Eq. (7) will be:

$$\begin{aligned}&(x_{O''} + \left(2e_0^2 + 2e_1^2 - 1\right)x''_{O'} + (2e_1e_2 - 2e_0e_3)y''_{O'} + (2e_1e_3 + 2e_0e_2)z''_{O'} - x_O)^2 \\ &\quad + (y_{O''} + (2e_1e_2 + 2e_0e_3)x''_{O'} + \left(2e_0^2 + 2e_2^3 - 1\right)y''_{O'} + (2e_2e_3 - 2e_0e_1)z''_{O'} - y_O)^2 \\ &\quad + (z_{O''} + (2e_1e_3 - 2e_0e_2)x''_{O'} + (2e_2e_3 + 2e_0e_1)y''_{O'} + \left(2e_0^2 + 2e_3^2 - 1\right)z''_{O'} - z_O)^2 - R_{\mathrm{w}}^2 = 0\end{aligned} \tag{10}$$

where the components of the origin point of the strut-fixed $O''x''y''z''$ frame $(x_{O''}, y_{O''}, z_{O''})$ and the Euler parameters are the unknown quantities. $(x''_{O'}, y''_{O'}, z''_{O'})$ are the components of the point O' in the $O''x''y''z''$ frame (fixed values).

In the same way, Eq. (8) will be:

$$\begin{aligned}&a_1(x_{O''} + \left(2e_0^2 + 2e_1^2 - 1\right)x''_{O'} + (2e_1e_2 - 2e_0e_3)y''_{O'} + (2e_1e_3 + 2e_0e_2)z''_{O'} - x_O) \\ &\quad + a_2(y_{O''} + (2e_1e_2 + 2e_0e_3)x''_{O'} + \left(2e_0^2 + 2e_2^2 - 1\right)y''_{O'} + (2e_2e_3 - 2e_0e_1)z''_{O'} - y_O) \\ &\quad + a_3(z_{O''} + (2e_1e_3 - 2e_0e_2)x''_{O'} + (2e_2e_3 + 2e_0e_1)y''_{O'} + \left(2e_0^2 + 2e_3^2 - 1\right)z''_{O'} - z_O) = 0\end{aligned} \tag{11}$$

where a_1, a_2, a_3 are the direction cosines (fixed values) of the vectors $\vec{\boldsymbol{u}}_{\mathrm{w}}$, the pivot axis of the wishbone.

4.2. Steering rod constraint equation

The steering rod is assumed as a spherical–spherical composite joint. Its analytical definition is that the distance between points C and D be equal the rod length (R_{s}) (Fig. 5).

$$\Phi^{\mathrm{ss}}(C, D, R_{\mathrm{s}}) = \vec{\boldsymbol{d}}^{\mathrm{T}}_{CD} \cdot \vec{\boldsymbol{d}}_{CD} - R_{\mathrm{s}}^2 = 0 \tag{12}$$

where $\vec{\boldsymbol{d}}_{CD}$ is:

$$\vec{\boldsymbol{d}}_{CD} = \vec{\boldsymbol{r}}_{O''} + [\mathbf{B}] \cdot \vec{s}^{\mathrm{T}}_{O''C} - \vec{\boldsymbol{r}}_D \tag{13}$$

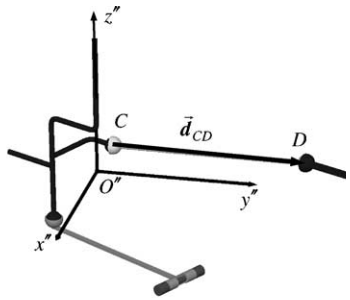

Fig. 5. Spherical–spherical composite joint.

Substituting Eq. (13) into Eq. (12) and expanding it the following expression is obtained:

$$\begin{aligned}&\left(x_{O''}+\left(2e_0^2+2e_1^2-1\right)x''_C+(2e_1e_2-2e_0e_3)y''_C+(2e_1e_3+2e_0e_2)z''_C-x_D\right)^2\\&\quad+\left(y_{O''}+(2e_1e_2+2e_0e_3)x''_C+\left(2e_0^2+2e_2^2-1\right)y''_C+(2e_2e_3-2e_0e_1)z''_C-y_D\right)^2\\&\quad+\left(z_{O''}+(2e_1e_3-2e_0e_2)x''_C+(2e_2e_3+2e_0e_1)y''_C+\left(2e_0^2+2e_3^2-1\right)z''_C-z_D\right)^2-R_s^2=0\end{aligned}\qquad(14)$$

where (x''_C, y''_C, z''_C) are the components of the point C in the $O''x''y''z''$ frame (fixed values). (x_D, y_D, z_D) are the components of the point D in the reference frame of the vehicle. The value of this components depends on the steering wheel position, one of the two degrees of freedom.

4.3. Strut constraint equations

The analytical definition of the strut joint is that the distance between points B and O'' be equal to a time-dependent length (L_{st}) and the vector defined by points B and O'' be orthogonal to $\vec{x}''$ and $\vec{y}''$ (Fig. 6).

The distance between points B and $O''(L_{st})$ is one of the two degrees of freedom and can be measured in a real case with a position sensor.

The constraint equations of the strut kinematic model can be written as:

$$\Phi^p(\vec{x}'', \vec{d}_{O''B}) = 0 \qquad (15)$$

$$\Phi^p(\vec{y}'', \vec{d}_{O''B}) = 0 \qquad (16)$$

$$\Phi^d(O'', B, L_{st}) = \vec{d}^{\mathrm{T}}_{O''B} \cdot \vec{d}_{O''B} - L_{st}^2 = 0 \qquad (17)$$

where $\vec{d}_{O''B}$ is:

$$\vec{d}_{O'B} = \begin{bmatrix} x_B \\ y_B \\ z_B \end{bmatrix} - \begin{bmatrix} x_{O''} \\ y_{O''} \\ z_{O''} \end{bmatrix} \qquad (18)$$

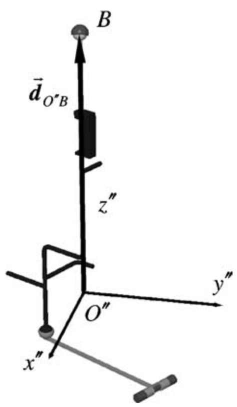

Fig. 6. Strut joint.

Expanding Eqs. (15)–(17) the following expressions are obtained ((19)–(21) respectively):

$$(2e_0^2 + 2e_1^2 - 1)(x_B - x_{O''}) + (2e_1e_2 + 2e_0e_3)(y_B - y_{O''}) + (2e_1e_3 - 2e_0e_2)(z_B - z_{O''}) = 0 \tag{19}$$

$$(2e_1e_2 - 2e_0e_3)(x_B - x_{O''}) + (2e_0^2 + 2e_2^2 - 1)(y_B - y_{O''}) + (2e_2e_3 + 2e_0e_1)(z_B - z_{O''}) = 0 \tag{20}$$

$$(x_B - x_{O''})^2 + (y_B - y_{O''})^2 + (z_B - z_{O''})^2 - L_{\mathrm{st}}^2 = 0 \tag{21}$$

4.4. Constraint equations of the McPherson kinematic model

The constraint equation system of each wheel will be:

$$\boldsymbol{\Phi}(\boldsymbol{q}, t) = \begin{bmatrix} \Phi^d(O', O, R_{\mathrm{w}}) \\ \Phi^p(\vec{\boldsymbol{u}}_{\mathrm{w}}, \vec{\boldsymbol{d}}_{OO'}) \\ \Phi^{\mathrm{ss}}(C, D, R_{\mathrm{s}}) \\ \Phi^p(\vec{\boldsymbol{x}}'', \vec{\boldsymbol{d}}_{O''B}) \\ \Phi^p(\vec{\boldsymbol{y}}'', \vec{\boldsymbol{d}}_{O''B}) \\ \Phi^d(O'', B, L_{\mathrm{st}}) \\ \Phi^{\mathrm{pe}} = e_0^2 + e_1^2 + e_2^2 + e_3^2 - 1 \end{bmatrix} = 0 \tag{22}$$

where Φ^{pe} is the Euler parameter normalization constraint.

Once the system of equations (22) has been solved the following variables, and therefore the transformation matrix of coordinates described in Section 3, are known:

$$\boldsymbol{q} = (x_{O''}, y_{O''}, z_{O''}, e_0, e_1, e_2, e_3) \tag{23}$$

The system of equations is solved using the iterative Newton–Raphson method.

5. Application of the kinematic model

5.1. Spatial positioning of the wheel—suspension geometry

Once the position and orientation of the movable reference frame has been determined, the direction vector of the wheel plane can be obtained (24). This will be parallel to the spin axis of the wheel (Fig. 7) and allows the determination of the characteristic geometry of the suspension system.

$$\vec{\boldsymbol{u}}_{wh} = \begin{bmatrix} u_{wh_x} \\ u_{wh_y} \\ u_{wh_z} \end{bmatrix} = [\mathbf{B}] \cdot \begin{bmatrix} u_{wh_{x''}} \\ u_{wh_{y''}} \\ u_{wh_{z''}} \end{bmatrix} \tag{24}$$

where $[u_{wh_{x''}}, u_{wh_{y''}}, u_{wh_{z''}}]$ are the components of the direction vector of the wheel plane expressed in the mobile system, fixed value. $\vec{\boldsymbol{u}}_{wh}$ is the direction vector of the wheel plane expressed in the vehicle reference.

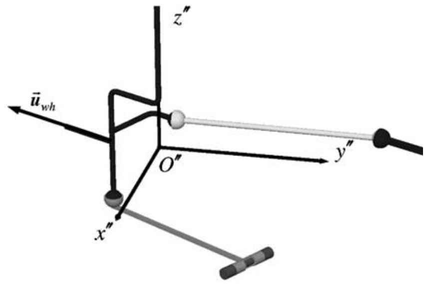

Fig. 7. Spin axis of the wheel.

The suspension geometry to be considered (kingpin, caster, camber and toe-in/out, in function of the various coordinates and wheel vector calculated) can be defined as:

$$\text{camber} = -\sin^{-1}\left(\frac{u_{wh_z}}{|\vec{\boldsymbol{u}}_{wh}|}\right) \tag{25}$$

$$\text{toe-in} = \sin^{-1}\left(\frac{u_{wh_x}}{\sqrt{(u_{wh_x})^2 + (u_{wh_y})^2}}\right) \tag{26}$$

$$\text{kingpin} = \text{tg}^{-1}\frac{y_B - y_{O'}}{z_B - z_{O'}} \quad \text{(right wheel)} \tag{27}$$

$$\text{kingpin} = \text{tg}^{-1}\frac{y_{O'} - y_B}{z_B - z_{O'}} \quad \text{(left wheel)} \tag{28}$$

$$\text{caster} = \text{tg}^{-1}\frac{x_{O'} - x_B}{z_B - z_{O'}} \tag{29}$$

In Eqs. (27)–(29) the components of the point O' in the vehicle reference frame are calculated using the following expression:

$$\begin{bmatrix} x_{O'} \\ y_{O'} \\ z_{O'} \end{bmatrix} = \begin{bmatrix} x_{O''} \\ y_{O''} \\ z_{O''} \end{bmatrix} + [\mathbf{B}] \cdot \begin{bmatrix} x''_{O'} \\ y''_{O'} \\ z''_{O'} \end{bmatrix} \tag{30}$$

5.2. Instantaneous axis of rotation of each wheel with respect to the body

The instantaneous axis of rotation of each wheel with respect to the body is defined as the intersection of the plane which contains the axis of rotation of the wishbone of the suspension and the point O', with the plane perpendicular to the line $O'B$ and which contains point B. Analytically this is represented with the following system of equations.

$$\left.\begin{array}{l}(x - x_O)v_x + (y - y_O)v_y + (z - z_O)v_z = 0 \\ (x - x_B)(x_B - x_{O'}) + (y - y_B)(y_B - y_{O'}) + (z - z_B)(z_B - z_{O'}) = 0\end{array}\right\} \tag{31}$$

where v_x, v_y, v_z are the components of a vector calculated by the expression:

$$\vec{\boldsymbol{v}} = \frac{\vec{\boldsymbol{d}}_{OO'}}{R_{\mathrm{w}}} \wedge \vec{\boldsymbol{u}}_{\mathbf{w}} = [v_x, v_y, v_z] \tag{32}$$

To calculate the swing arm equivalent, it is necessary to draw the perpendicular to the instant axis of rotation, which passes through the point of contact of the wheel with the ground. This point, the point of tangency between the effective circumference of the wheel and the ground, is calculated solving the following system of equations:

$$\begin{bmatrix} \Phi^p(\vec{\boldsymbol{u}}_{wh}, \vec{\boldsymbol{d}}_{O_rP}) \\ \Phi^d(\vec{\boldsymbol{d}}_{O_rP}, R_{wh}) \\ \Phi^p(\vec{\boldsymbol{v}}_{wh}, \vec{\boldsymbol{d}}_{O_rP}) \end{bmatrix} = 0 \tag{33}$$

where $\vec{\boldsymbol{v}}_{wh}$ is the vector:

$$\vec{\boldsymbol{v}}_{wh} = -u_{wh_y}\vec{\boldsymbol{i}} + u_{wh_x}\vec{\boldsymbol{j}} \tag{34}$$

All the vectors must be expressed in the road reference frame.

5.3. Front roll axis

Starting from the instantaneous axis of rotation for each of the wheels, the roll axis is calculated as the intersection of the plane which contains the instant axis of the right wheel, and which passes through its point of contact with the plane which contains the instant axis calculated for the left wheel and its corresponding contact with the rolling surface (Fig. 8).

5.4. Modification of the height of the knuckle due to the rotation of the steering wheel

As can be seen in Fig. 9 the centre of the wheel O_R describes the circumference which forms an angle with the ground. On turning the wheel through the effect of the compression of the suspension or through the turning of the steering wheel, a variation in the height of the knuckle is produced, and consequently in the point B with respect to the ground.

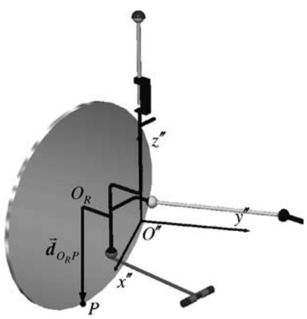

Fig. 8. Vector of the contact point.

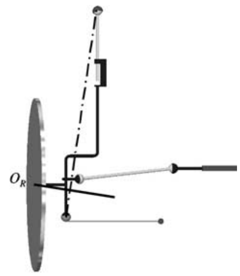

Fig. 9. Circumference which describes the centre of the wheel.

To calculate this variation it is necessary to calculate the position of the centre of the wheel O_R and the point of contact of the wheel with the ground.

6. Development of the software, validation and application of the model

To solve the equations and the representation of the variation of the steering and suspension geometry, the programme MATLAB® and its interactive tool for modelisation, Simulink®, were employed. MATLAB® has been chosen since it represents an integrated environment which combines numeric computation, advanced graphics, visualisation and a high-level programming language [14].

The model presented for the *McPherson* front suspension requires a series of geometric data such as the coordinates of the *McPherson* strut mount (point *B*), the joints of the wishbone to the body, and the anchor points of the steering rack. Other data are references to the geometry of the knuckle. Finally, the model needs the length of the strut and the turn of the steering wheel at each moment. The complete list is presented in Appendix A.

6.1. Validation of the model

In order to test the solution of the MATLAB® model, the results were contrasted with the measurements carried out on a real, instrumented vehicle.

The contrast process consisted of the measurement in the real vehicle of the variation of the steering and suspension geometries with the length of the damper and the steering angle. Potentiometric wire sensors were employed to measure the length of the damper and a rotary potentiometer to measure the steering angle. To measure the steering and suspension geometry Culmen-opto-plus, mod. 302 HD, optical measuring equipment was used.

One of the procedures used to measure the variation consisted of raising the vehicle parallel to the ground from rest position to that in which the wheels were in the air. Another one consisted of turning the steering wheel for different body positions. Some of the graphs obtained compared with those calculated through the model are shown in Figs. 10–13.

A small difference can be appreciated in these figures between the model and the measurements, this being essentially a function of the errors of measurement associated with the instruments used.

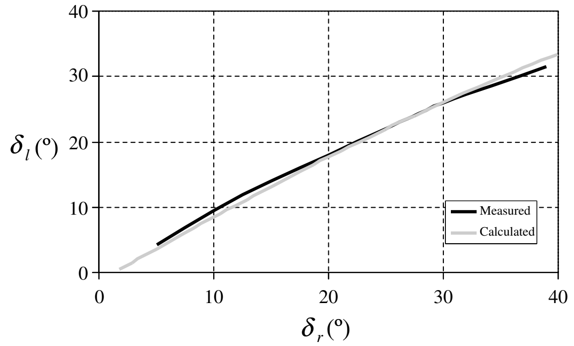

Fig. 10. Left steering wheel angle vs. right steering wheel angle measured in the vehicle and calculated in the model.

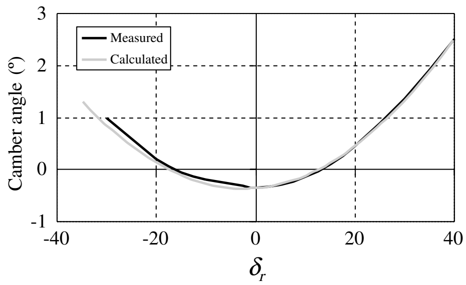

Fig. 11. Camber angle (right wheel) measured in the vehicle and calculated in the model vs. wheel angle.

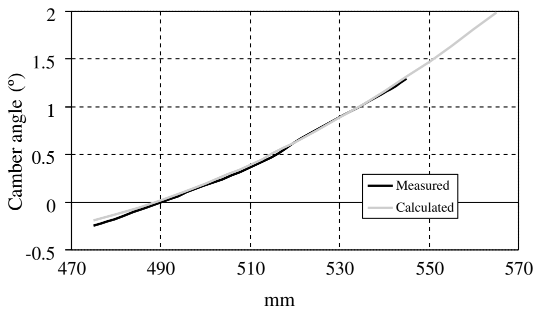

Fig. 12. Camber angle (right wheel) measured in the vehicle and calculated in the model vs. the length of damper (McPherson strut).

6.2. Results and analysis of the vehicle

Through the model it is possible to obtain the complete three-dimensional geometric characterisation of the system. As an example, various graphs referring to the variation of certain important dimensions are shown in Figs. 14 and 15.

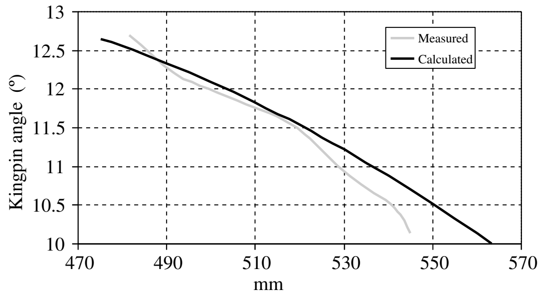

Fig. 13. Kingpin inclination measured in the vehicle and calculated in the model vs. the length of damper (McPherson strut).

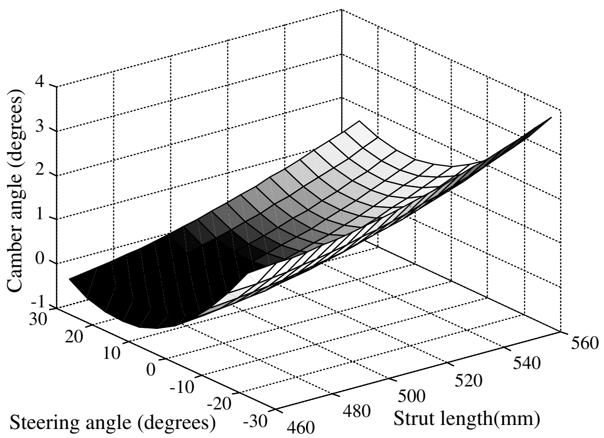

Fig. 14. Surface of variation of the angle of camber vs. the length of the damper and with the turn of wheel.

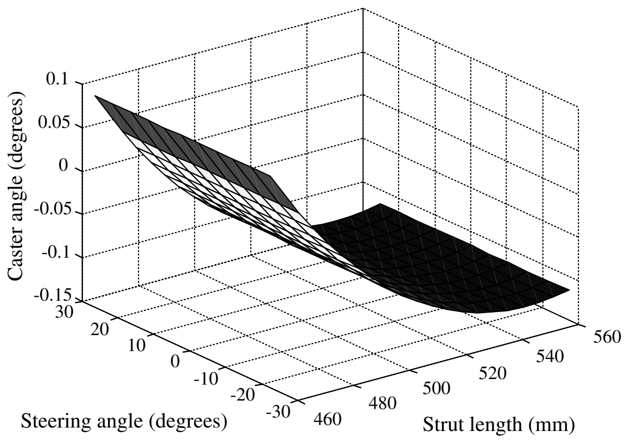

Fig. 15. Surface of variation of the angle of caster vs. the length of the damper and with the turn of wheel.

6.3. Roll centre

An important parameter in order to improve the cornering behaviour of a vehicle is the height of the roll centre. Using the model we developed, the position of the roll centre was calculated with the vehicle in rest position, and its variation due to dynamic forces.

Fig. 16 shows the variation of roll centre height with a vertical movement of the vehicle parallel to the ground, with a variation in the lengths of the strut between 460 and 600 mm.

The second case consisted of considering the roll movement of the body, starting from the rest position, a length of 530 mm in both dampers, and rolling towards the left and then the right. For the roll towards the left it is assumed that the right damper goes from 530 to 600 mm in the same time in which the left goes from 530 to 460 mm in length. The results can be seen in Fig. 17.

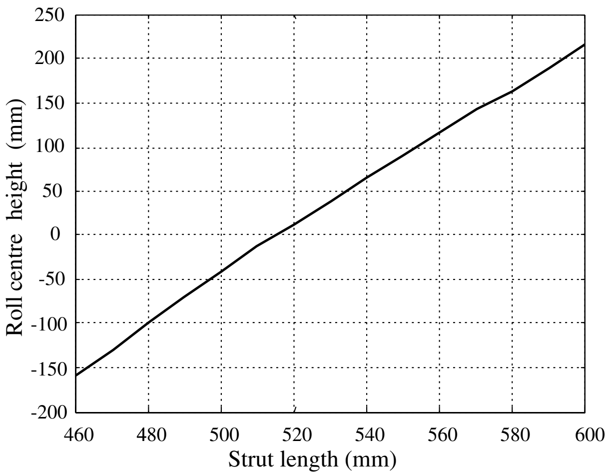

Fig. 16. Height of the roll centre for a movement parallel to the body.

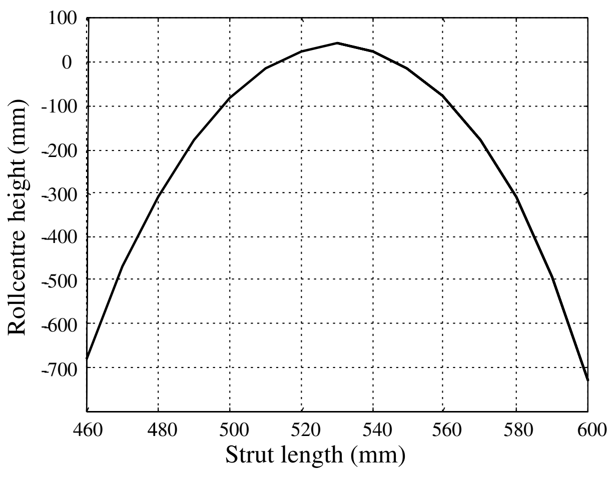

Fig. 17. Roll centre height for the roll movement of the body.

7. Conclusions

A kinematic model has been developed for the most commonly used type of steering suspension, and a computation programme has been implemented which facilitates the resolution for any user. It is a flexible model which can be applied to any McPherson configuration.

With this model it is possible to calculate the variation in the suspension geometry as a function of the travel of the strut and of the turn of the steering wheel. Since the geometry is a determining factor in the stability and handling, the model allows the optimisation of the suspension mechanism. This can be carried out during the design phase, since the most adequate position of the joints of the links, their length, etc., can be determined easily.

At the same time, the model permits optimisation once the vehicle has been manufactured, as is the case with competition vehicles, thanks to which the calculation of the ideal suspension settings is facilitated.

Finally, it is worth pointing out that the model can be applied to a vehicle with instrumented suspension and steering, allowing us to know the position of the wheel and the steering and suspension geometry in real time.

Acknowledgement

Thanks to Robin Walker for his revision of the English.

Appendix A. Data of the vehicle analysed

Characteristic dimensions of the steering mechanism (vehicle reference)

Dimension	Value
Tie rod right/left	338 mm
Rack-and-pinion ratio	48 mm/rev
Distance Q–C, steer angle = 0	125 mm

Characteristic dimensions of the suspension (vehicle reference)

Coordinate (vehicle reference)		Value (mm)
x_B	Right/left	1100
y_B	Right/left	−550.5/550.5
z_B	Right/left	360
x_{R_1}	Right/left	1046.1
y_{R_1}	Right/left	−351.5/351.5
z_{R_1}	Right/left	−310
x_{R_2}	Right/left	796
y_{R_2}	Right/left	−310.1/310.1
z_{R_2}	Right/left	−310
x_Q	Right/left	926

(*continued on next page*)

Appendix A (*continued*)

Coordinate (vehicle reference)		Value (mm)
y_Q	Right/left	−202.5/202.5
z_Q	Right/left	−200

Characteristic dimensions of the suspension (knuckle reference)

Coordinate (knuckle reference)		Value (mm)
x''_C	Right/left	−150
y''_C	Right/left	0
z''_C	Right/left	0
x''_{O_R}	Right/left	−94.77
y''_{O_R}	Right/left	−125.09/125.09
z''_{O_R}	Right/left	−15.93
$x''_{O'}$	Right/left	−59.43
$y''_{O'}$	Right/left	−78.44/78.44
$z''_{O'}$	Right/left	−94.42
x''_N	Right/left[a]	−33.92
y''_N	Right/left[a]	−44.77/44.77
z''_N	Right/left[a]	−15.58

Characteristic dimensions of the wishbone

Distances (Fig. 18)	Value (mm)
d_1	254
d_2	325
d_3	475

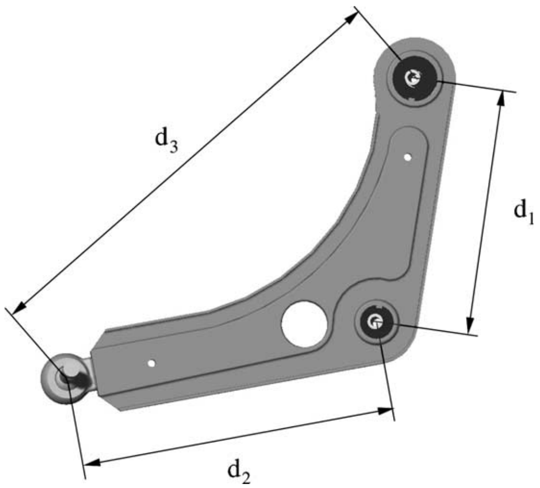

Fig. 18. Wishbone.

References

[1] J. Reimpell, H. Stoll, The Automotive Chassis: Engineering Principles, Ed. Arnold, London, 1998.
[2] I. Esat, Genetic algorithm-based optimization of a vehicle suspension system, Int. J. Vehicle Des. 21 (2/3) (1999) 148–160.
[3] M. Kaminaga, M. Murata, Y. Tateishi, Factoring nonlinear kinematics into new suspension design: a CAE approach to vehicle roll dynamics, Nissan Motor Co., Ltd., SAE paper no. 940871, 1994.
[4] J. Kang, J. Yun, J. Lee, T. Tak, Elastokinematic analysis and optimization of suspension compliance characteristics, Seoul National University and Kangwon National University, SAE paper no. 970104, 1997.
[5] M. Raghavan, An atlas of linkages for independent suspensions, Power Systems Research Department, General Motors Research Labs., SAE paper no. 911925, 1991.
[6] F. Montoya, Cinemá tica y Dinámica de Mecanismos 3D, Universiad de Valladolid, 1997.
[7] S. Song, X. Gao, Movility equation and the solvability of joint forces/torques in dynamic analysis, J. Mech. Des., ASME 114 (1992) 257–262.
[8] H.Y. Kang, C.H. Suh, Synathesis and analysis of spherical–cylindrical (SC) link in the mcpherson strut suspension mechanism, J. Mech. Des. 116 (1994) 599–606.
[9] J. Haug Edward, Computer aided Kinematic and Dynamics in Mechanical Systems, Ed. Allyn and Bacon, Massachusetts, 1989.
[10] R. Serban, J.S. Freeman, Identification and identifiability of unknown parameters in multibody dynamic systems, Multibody Syst. Dyn. J. 5 (4) (2001) 335–350.
[11] R. Serban, E. Haug, Globally independent coordinates for real-time vehicle simulation, J. Mech. Des., ASME 122 (4) (2000) 575–582.
[12] P.E. Nikravesh, R.A. Wehage, O.K. Kwon, Euler parameters in computational kinematics and dynamics. Part 1, Trans. ASME 107 (1985) 358–365.
[13] D.M.A. Lee et al., A real-time multibody vehicle dynamic analysis method using suspension composite joints, Int. J. Vehicle Des. 24 (3/2) (2000) 259–273.
[14] K. Connair, M. Bodie, P. Chaumette, Development of a common vehicle model for chassis control design, SAE paper no. 1999-01-0732, 1999.